Parameter-Less Fault Locator for Double-Circuit Transmission Line Using Two-Terminal Unsynchronized Measurements

Ahmed Saber, H. H. Zeineldin, *Senior Member, IEEE*, and Ehab F. El-Saadany, *Fellow, IEEE*

***Abstract*—This paper develops a parameter-free fault location (FL) method for double-circuit transmission lines utilizing pre- and post-fault unsynchronized current and voltage measurements. Firstly, the FL equation is deduced for normal-shunt and non-identical inter-circuit faults (involving different phases in both circuits). The FL equation relies on equating the voltage phasors' difference between identical phases in the two circuits at the FL without utilizing the line parameters and synchronization angle between both line terminals. Next, the FL equation is deduced for identical inter-circuit faults (involving identical phases in both circuits) utilizing pre- and post-fault measurements, where a new method is introduced to obtain the pre-fault synchronization angle and line shunt-admittance relying on pre-fault data. Besides, it considers different synchronism mismatch in the pre- and post-fault data. To distinguish identical inter-circuit faults from other fault types, the absolute difference, between post-fault currents of identical phases in both circuits at each line terminal, is employed. PSCAD/EMTDC software is used for modeling the IEEE 39-bus system to evaluate the proposed method for various fault resistances, locations, fault types, and measurement errors. In addition, the developed method offers solid performance against evolving faults and different loading conditions. Moreover, it remains applicable when one of the two circuits is out-of-service.**

***Index Terms*—Transmission line, line parameters, fault location.**

I. Introduction

Estimating the fault location for double-circuit transmission lines, which are widely used in power systems, is much more complex and challenging than fault allocation for single-circuit transmission lines due to the mutual couplings and potential of faults between both circuits. The principles and the various FL techniques for single-circuit lines and double-circuit lines are provided in [1], involving traveling-wave based [2], [3], knowledge based (data driven) [4], [5], time-domain based [6], [7], and power frequency-domain based techniques. Traveling wave based techniques analyze the arrival traveling wave at line terminals [2], [3]. However, these techniques are more expensive and complex since they rely on a high sampling frequency and may fail in detecting the wave-front in the case of high impedance faults. Knowledge based techniques estimate the FL utilizing the available measurements [4], [5]. However, these techniques require numerous training data for a specific line under different fault scenarios to perform initially the training process. The actual training data is typically not available for physical power systems, and these techniques cannot be applied for a new line without implementing a new training process. Time-domain based techniques employ different line models and short data windows to estimate the FL [6], [7]. These techniques utilize both instantaneous voltage and current measurements, and their accuracy are highly affected by the uncertainties in line parameters. Power frequency-domain based techniques are widely used in transmission networks due to phasor measurements' availability in practical substations and power plants. Besides, the FL calculations are less complicated compared to other techniques because the FL equations are derived in algebraic approach in phasor domain.

Based on the availability of the measurements and communication links, power frequency-domain based schemes can be categorized into single- and double- terminal FL schemes. One-terminal FL schemes are vastly used in transmission systems as they can be easily implemented and are more economical. However, their precision degrades due to several factors, such as the unknown grid impedance at remote line terminal, load current, and fault resistance, since local data are only utilized for deriving the FL equation [8], [9]. On the other hand, double-end techniques have higher accuracy due to the availability of the measurements from both line terminals. However, some of these techniques rely on synchronized data, which require installing additional equipment [10]. Thus, different FL techniques have been proposed using only the unsynchronized measurements [11], [12]. Besides, the line parameters are practically exposed to continuous changes because of loading and weather circumstances, degrading the FL precision.

Manuscript received 4 October 2023; revised 28 January 2024, 26 April 2024, and 13 June 2024; accepted 25 June 2024. Date of publication 1 July 2024; date of current version 25 September 2024. This work was supported in part by the Advanced Power and Energy Center APEC, under Grant RCII-03-2018, in part by Khalifa University, Abu Dhabi, UAE, and in part by the ASPIRE through the ASPIRE Virtual Research Institute (VRI) Program, under Award VRI20-07. ASPIRE is part of the Advanced Technology Research Council located in Abu Dhabi, UAE. Paper no. TPWRD-01390-2023. *(Corresponding author: Ahmed Saber.)*

Ahmed Saber is with Cairo University, Giza 12613, Egypt, and also with Khalifa University, Abu Dhabi 22219, UAE (e-mail: a_saber_86@cu.edu.eg).

H. H. Zeineldin is with Advanced Power and Energy Center (APEC), Department of Electrical Engineering, Khalifa University, Abu Dhabi 22219, UAE, and also with Electric Power Engineering Department, Cairo University, Giza 12613, Egypt (e-mail: hatem.zeineldin@ku.ac.ae).

Ehab F. El-Saadany is with Advanced Power and Energy Center (APEC), Electrical Engineering and Computer Science Department, Khalifa University, Abu Dhabi 22219, UAE.

Color versions of one or more figures in this article are available at https://doi.org/10.1109/TPWRD.2024.3420087.

Digital Object Identifier 10.1109/TPWRD.2024.3420087

To overcome the problem of the inaccurate line parameters, different parameter-free FL methods have been introduced in the literature [13], [14], [15], [16], [17], [18], [19], [20], [21], [22], [23], [24], [25], [26], [27], [28], [29]. In [13], the pre- and post-fault unsynchronized current and voltage data at line terminals are utilized to determine the line parameters and locate the faults on a single-circuit line. However, this technique is applicable only for transposed lines, and there is a concern over its convergence because it is based on least-square algorithm. The technique in [13] has been extended in [14] for untransposed single-circuit lines. Although FL accuracy has been improved, synchronism mismatch in the pre- and post-fault data does not taken into account. In [15], [16], [17], [18], [19], FL techniques have been proposed for single-circuit lines using synchronized current and voltage data. However, the techniques [15], [16], [17] relies on the lumped line parameters, yet ignoring the line shunt admittance, and being applied only for transposed lines, while the techniques [18], [19], have turned the problem into an optimization problem, which may encounter divergence problems. In [20], a technique is introduced based on the synchronized data for untransposed single-circuit lines, where it is not accounted for the GPS signal loss. Iterative [21], [22], [23] and non-iterative [24], [25], [26], [27] fault location methods have been proposed, which are only applicable for single-circuit lines and transposed double circuit lines. In [28], unsynchronized current phasors are employed to locate the faults on an untransposed double-circuit line, where the unknown variables in the derived FL equation include the synchronization angle (SA) between line terminals and the fault distance. This technique is a parameter-free, and the identification of the faulted phases is not required. However, it is not applicable for identical inter-circuit faults, which involve identical phases in different circuits. In [29], unsynchronized positive-sequence current and voltage phasors are employed to locate the faults on a double-circuit line. However, ignoring the line untransposition and capacitance has degraded its accuracy. In [30], unsynchronized data are utilized to estimate the FL on a double-circuit line. The FL is determined relying on unscented Kalman filter based state estimation algorithm. However, different unknown variables, such as the fault distance, line parameters, SA, and fault resistance, are required to be estimated, leading to a highly nonlinear problem. Therefore, it is more prone to divergence problems. In [31], a parameter-free technique is employed to locate the faults on transposed double-circuit lines using unsynchronized positive-sequence current phasors. However, it is not applicable for identical inter-circuit faults. Based on the above discussion, it is evident that the parameter-free FL techniques outlined in the literature for double-circuit lines have some limitations. The FL technique in [28] and [31] are not suitable for identical inter-circuit faults, whereas the technique in [29] are inaccurate due to ignoring line untransposition and capacitance. In addition, the technique in [30] is prone to divergence issues.

In this research, a FL method is proposed for double-circuit transmission lines using pre- and post-fault unsynchronized measurements at both line terminals. Firstly, the unsynchronized currents at both terminals are utilized to derive an analytical FL equation for normal-shunt and non-identical inter-circuit faults. The derived equation relies on the π model and equating the voltage phasors' difference between identical phases in the two circuits at the FL. Additionally, the SA between both line terminals and line parameters are not required. Next, the FL equation is developed based on the π line model without the need for line parameters for identical inter-circuit faults, which involve identical phases in the two circuits. The pre- and post-fault measurements as well as the SA are required. Thus, the pre-fault SA and the line-shunt admittance are estimated utilizing pre-fault data, where its derivation relies on the fact that the angle of the line-shunt admittance is equal to 90°. The developed method is evaluated via PSCAD/EMTDC software. Various scenarios are conducted, including all fault types, fault locations and resistances, and measurement errors. The contributions of this paper are:

- A parameter-free FL approach is proposed considering all fault types.
- The derived fault location equation in [28] contains two unknown variables; the SA and fault distance. The proposed steps for FL derivation further simplify the FL equation, where it is demonstrated that there is no requirement to estimate the SA, and the fault location can be directly and effortlessly calculated.
- The proposed approach determines the SA based on only pre-fault data, which can also be used for other purposes beyond estimating the FL. Furthermore, the proposed technique can be applied for identical inter-circuit faults, where the FL technique in [28] fails in such cases.
- The developed FL approach considers different synchronism mismatch in the pre- and post-fault data [26].
- The proposed approach remains applicable when one of the two circuits is out-of-service, unlike that in [28] and [31].

The article is arranged as follows. In Section II, the developed FL method is deduced for normal-shunt and non-identical inter-circuit faults as well as identical inter-circuit faults. In Section III, the outcomes are shown for PSCAD simulation. Lastly, Section IV concludes the article.

II. Developed Fault Location Method

In part II.A, the FL equation is developed relying on the π model for normal-shunt and non-identical inter-circuit faults using unsynchronized phase currents at both line terminals. In Part II.B, the FL equation is developed for identical inter-circuit faults employing pre- and post-fault measurements at both line terminals and the estimated SA, which is inferred by relying on the fact that the angle of the line-shunt admittance is equal to 90°. In the following formulation, it is considered that the two circuits are connected at the same buses at both line terminals.

A. *Formulation of the FL Equation for Normal-Shunt and Non-Identical Inter-Circuit Faults*

In [28], the derived FL equation contains two unknown variables; the SA between both line terminals and the fault distance. This technique is extended here; where it is proved that the SA is not needed to be estimated. In addition, only the phase currents at both line sides are needed for deriving the FL equation. However, as shown later in this part, this developed equation fails only

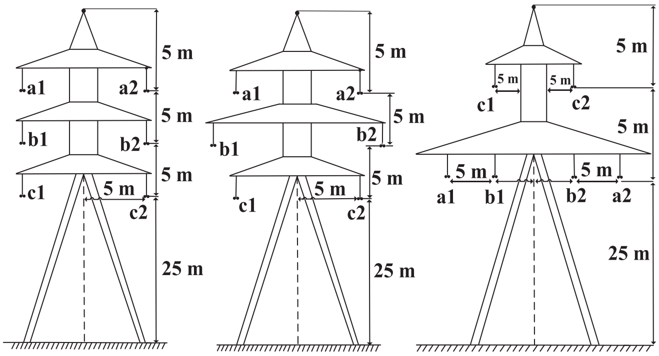

Fig. 1. Typical tower layout for 220 kV double-circuit line.

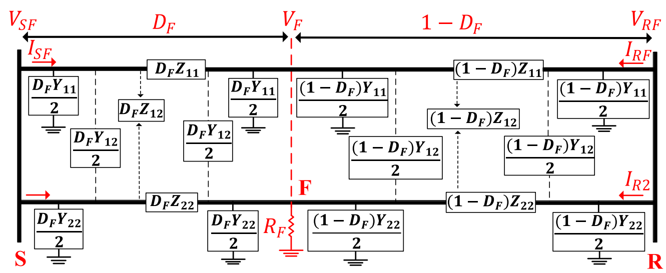

Fig. 2. Double-circuit line representation during fault conditions (π line model).

when an identical inter-circuit fault occurs on identical phases in the two circuits.

In Fig. 1, the typical tower layouts are shown for the double-circuit line, where 6×6 series impedance matrix ($\boldsymbol{Z}_{SR}$) and 6×6 shunt admittance matrix ($\boldsymbol{Y}_{SR}$) can be represented as:

$$[\boldsymbol{Z}_{SR}] = \begin{bmatrix} z_{a1,a1} & z_{a1,b1} & z_{a1,c1} & z_{a1,a2} & z_{a1,b2} & z_{a1,c2} \\ z_{b1,a1} & z_{b1,b1} & z_{b1,c1} & z_{b1,a2} & z_{b1,b2} & z_{b1,c2} \\ z_{c1,a1} & z_{c1,b1} & z_{c1,c1} & z_{a1,c2} & z_{c1,b2} & z_{c1,c2} \\ z_{a2,a1} & z_{a2,b1} & z_{a2,c1} & z_{a2,a2} & z_{a2,b2} & z_{a2,c2} \\ z_{b2,a1} & z_{b2,b1} & z_{b2,c1} & z_{b2,a2} & z_{b2,b2} & z_{b2,c2} \\ z_{c2,a1} & z_{c2,b1} & z_{c2,c1} & z_{c2,a2} & z_{c2,b2} & z_{c2,c2} \end{bmatrix} \tag{1}$$

$$[\boldsymbol{Y}_{SR}] = \begin{bmatrix} y_{a1,a1} & y_{a1,b1} & y_{a1,c1} & y_{a1,a2} & y_{a1,b2} & y_{a1,c2} \\ y_{b1,a1} & y_{b1,b1} & y_{b1,c1} & y_{b1,a2} & y_{b1,b2} & y_{b1,c2} \\ y_{c1,a1} & y_{c1,b1} & y_{c1,c1} & y_{c1,a2} & y_{c1,b2} & y_{c1,c2} \\ y_{a2,a1} & y_{a2,b1} & y_{a2,c1} & y_{a2,a2} & y_{a2,b2} & y_{a2,c2} \\ y_{b2,a1} & y_{b2,b1} & y_{b2,c1} & y_{b2,a2} & y_{b2,b2} & y_{b2,c2} \\ y_{c2,a1} & y_{c2,b1} & y_{c2,c1} & y_{c2,a2} & y_{c2,b2} & y_{c2,c2} \end{bmatrix} \tag{2}$$

where a_1, b_1, c_1, a_2, b_2, and c_2 represent the phases of both circuits. In general, both circuits on either side of the tower are typically identical to each other. The 3×3 upper left side of $\boldsymbol{Z}_{SR}$ is equal to the 3×3 lower right side of $\boldsymbol{Z}_{SR}$, while the 3×3 lower left side of $\boldsymbol{Z}_{SR}$ is equal to the 3×3 upper right side of $\boldsymbol{Z}_{SR}$. This is also applicable for $\boldsymbol{Y}_{SR}$.

In Fig. 2, a generic fault on the double-circuit line (*S*-*R*) at a fault distance (D_F) away from end S is shown considering the π line model. The phase voltages in the phase-domain at the fault point ($\boldsymbol{V}_F$) is written utilizing the unsynchronized data at line terminals:

$$[\boldsymbol{V}_F] = \left[1 + \frac{[\boldsymbol{Z}_{SR}]\,[\boldsymbol{Y}_{SR}]\,{D_F}^2}{2}\right] [\boldsymbol{V}_{SF}]\; e^{j\delta} - D_F\,[\boldsymbol{Z_{SR}}]\,[\boldsymbol{I}_{SF}]\; e^{j\delta} \tag{3}$$

$$[\boldsymbol{V}_F] = \left[1 + \frac{[\boldsymbol{Z}_{SR}]\,[\boldsymbol{Y}_{SR}]\,(1-D_F)^2}{2}\right] [\boldsymbol{V}_{RF}] - (1-D_F)\,[\boldsymbol{Z}_{SR}]\,[\boldsymbol{I}_{RF}] \tag{4}$$

$$\boldsymbol{V}_{SF} = \begin{bmatrix} V_{SF,a1} & V_{SF,b1} & V_{SF,c1} & V_{SF,a2} & V_{SF,b2} & V_{SF,c2} \end{bmatrix}^T \tag{5}$$

$$\boldsymbol{V}_{RF} = \begin{bmatrix} V_{RF,a1} & V_{RF,b1} & V_{RF,c1} & V_{RF,a2} & V_{RF,b2} & V_{RF,c2} \end{bmatrix}^T \tag{6}$$

$$\boldsymbol{I}_{SF} = \begin{bmatrix} I_{SF,a1} & I_{SF,b1} & I_{SF,c1} & I_{SF,a2} & I_{SF,b2} & I_{SF,c2} \end{bmatrix}^T \tag{7}$$

$$\boldsymbol{I}_{RF} = \begin{bmatrix} I_{RF,a1} & I_{RF,b1} & I_{RF,c1} & I_{RF,a2} & I_{RF,b2} & I_{RF,c2} \end{bmatrix}^T \tag{8}$$

where $\boldsymbol{I}_{SF}$ and $\boldsymbol{I}_{RF}$ are, respectively, the post-fault phase currents at terminals S and R. $\boldsymbol{V}_{SF}$ and $\boldsymbol{V}_{RF}$ are, respectively, the post-fault phase voltages at line terminals (*S* and *R*). The symbol "T" refers to the transpose of the voltage or the current vector, while the symbol "δ" is the SA between both terminals *S* and *R*. As the voltage phasors at line sides ($\boldsymbol{V}_{SF}$ and $\boldsymbol{V}_{RF}$) of identical phases of the two circuits are equal, the differential components of ($\boldsymbol{V}_{SF}$ and $\boldsymbol{V}_{RF}$) is written as:

$$\begin{bmatrix} V_{SF,a1} - V_{SF,a2} \\ V_{SF,b1} - V_{SF,b2} \\ V_{SF,c1} - V_{SF,c2} \end{bmatrix} = \begin{bmatrix} V_{RF,a1} - V_{RF,a2} \\ V_{RF,b1} - V_{RF,b2} \\ V_{RF,c1} - V_{RF,c2} \end{bmatrix} = \begin{bmatrix} 0 \\ 0 \\ 0 \end{bmatrix} \tag{9}$$

Considering (9), the same phases of both circuits in (3) and (4) are subtracted from each other:

$$\begin{bmatrix} V_{F,a1} - V_{F,a2} \\ V_{F,b1} - V_{F,b2} \\ V_{F,c1} - V_{F,c2} \end{bmatrix} = -D_F\,[\Delta \boldsymbol{Z}_{SR}] \begin{bmatrix} I_{SF,a1} - I_{SF,a2} \\ I_{SF,b1} - I_{SF,b2} \\ I_{SF,c1} - I_{SF,c2} \end{bmatrix} e^{j\delta} \tag{10}$$

$$\begin{bmatrix} V_{F,a1} - V_{F,a2} \\ V_{F,b1} - V_{F,b2} \\ V_{F,c1} - V_{F,c2} \end{bmatrix} = -(1-D_F)\,[\Delta \boldsymbol{Z}_{SR}] \begin{bmatrix} I_{RF,a1} - I_{RF,a2} \\ I_{RF,b1} - I_{RF,b2} \\ I_{RF,c1} - I_{RF,c2} \end{bmatrix} \tag{11}$$

$$[\Delta \boldsymbol{Z}_{SR}] = \begin{bmatrix} z_{a1,a1} - z_{a1,a2} & z_{a1,b1} - z_{b1,a2} & z_{a1,c1} - z_{c1,a2} \\ z_{b1,a1} - z_{a1,b2} & z_{b1,b1} - z_{b1,b2} & z_{b1,c1} - z_{c1,b2} \\ z_{c1,a1} - z_{a1,c2} & z_{c1,b1} - z_{b1,c2} & z_{c1,c1} - z_{c1,c2} \end{bmatrix} \tag{12}$$

The derivation for the results of the right-hand side in (10) and (11) are given in the appendix. Substituting (11) into (10):

$$D_F \begin{bmatrix} I_{SF,a1} - I_{SF,a2} \\ I_{SF,b1} - I_{SF,b2} \\ I_{SF,c1} - I_{SF,c2} \end{bmatrix} e^{j\delta} = (1-D_F) \begin{bmatrix} I_{RF,a1} - I_{RF,a2} \\ I_{RF,b1} - I_{RF,b2} \\ I_{RF,c1} - I_{RF,c2} \end{bmatrix} \tag{13}$$

The unknown variables in (13) are D_F and δ. Considering only the magnitudes in (13), the unknown δ is eliminated:

$$D_F \times \begin{bmatrix} |I_{SF,a1} - I_{SF,a2}| \\ |I_{SF,b1} - I_{SF,b2}| \\ |I_{SF,c1} - I_{SF,c2}| \end{bmatrix} = (1 - D_F) \times \begin{bmatrix} |I_{RF,a1} - I_{RF,a2}| \\ |I_{RF,b1} - I_{RF,b2}| \\ |I_{RF,c1} - I_{RF,c2}| \end{bmatrix} \tag{14}$$

where $|\,|$ refers to the absolute value. Rearranging (14) and taking the summation of the vector elements:

$$D_F = \frac{\sum_{\forall\, x\, \in\, \{a,b,c\}} \left(|I_{RF,x1} - I_{RF,x2}|\right)}{\sum_{\forall\, x\, \in\, \{a,b,c\}} \left(|I_{SF,x1} - I_{SF,x2}| + |I_{RF,x1} - I_{RF,x2}|\right)} \tag{15}$$

The only unknown variable in (15) is the fault distance (D_F). It is clear that (15) does not rely on the line parameters. Besides, it is applicable for all fault types without the need for identifying the faulted phases. In addition, only the unsynchronized phase currents at line terminals are needed. On the other hand, as shown in (15), it will not be applicable when an identical inter-circuit fault occurs since the currents of both circuits are identical at each line terminal. To overcome this problem, the FL equation in Part II.B is proposed to be applied to identical inter-circuit faults.

It is worth highlighting that the contributions of the proposed method presented in this subsection compared to [28], are as follows:

- The FL equation derived in [28] involves two unknown variables: the SA between line terminals and fault distance. The additional steps in (14) and (15) further simplified the FL equation. Hence, there is no need to estimate the SA; instead, the fault distance is easily and directly calculated using (15).
- In Section III-I, the developed FL method is compared with [28]. It was observed that, for non-ground faults, the developed FL method is more accurate than that in [28]. This is due to the fact that the FL in [28] is obtained in the sequence-domain, where either the positive, negative, or zero-sequence components can be utilized in the case of un-transposed double-circuit lines. Conversely, the developed FL method is formulated in the phase-domain, combining all phases together as depicted in (15), resulting in more accurate results.
- The FL method in [28] is not applicable when an identical inter-circuit fault occurs on the same phases in both circuits. As mentioned before, to address this issue, the FL equation is derived in Part II.B for handling identical inter-circuit faults.
- The FL method in [28] is ineffective when one of the two circuits is out of service. In contrast, the developed FL method remains applicable, as derived in Part II.B and demonstrated in the results presented in Part III.H.
- The developed FL method introduces a new approach to obtain the pre-fault SA using pre-fault data, as shown in (23). This can serve additional purposes beyond estimating the FL.

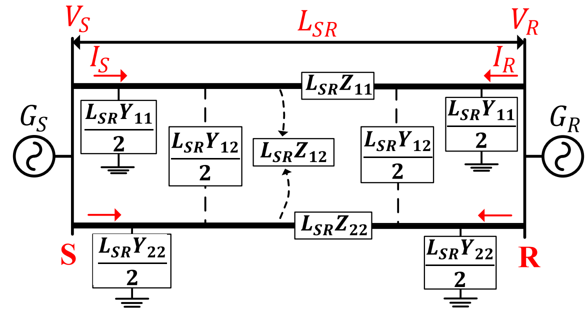

Fig. 3. Double-circuit line representation during normal conditions.

- A new technique is introduced to calculate the SA using only pre-fault data without requiring line parameters. This technique can also be used for other purposes beyond FL estimation.

B. FL Formulation for Identical Inter-Circuit Faults

In the case of the identical inter-circuit faults, the number of unknown line parameters is equal to that in the case of normal-shunt faults and non-identical inter-circuit faults. However, the number of equations in the case of the identical inter-circuit faults is equal to half the number of equations in the case of normal-shunt faults and non-identical inter-circuit faults because the voltages and currents of both circuits are identical in the case of the identical inter-circuit faults. Thus, this reduction in the equations further complicates the fault location problem. The proposed FL is developed without the need for the line parameters utilizing both pre- and post-fault measurements. It relies on the π model ignoring the mutual-admittance between different phases. As the SA is initially required, a new technique is firstly introduced to estimate the SA relying on pre-fault current and voltage measurements. The developed method relies on the fact that the angle of the line-shunt admittance equals 90°.

The double-circuit line is represented in Fig. 3 using the π model. The line length is denoted by L_{SR}. In normal conditions, the relations between the pre-fault currents ($\boldsymbol{I}_S$ and $\boldsymbol{I}_R$) in the phase-domain is written as:

$$\left\{[\boldsymbol{I}_S] - \frac{1}{2}[\boldsymbol{Y}_{SR}][\boldsymbol{V}_S]\right\} e^{j\delta} = -\left\{[\boldsymbol{I}_R] - \frac{1}{2}[\boldsymbol{Y}_{SR}][\boldsymbol{V}_R]\right\} \tag{16}$$

Rearranging (16):

$$\left[\boldsymbol{I}_S + \boldsymbol{I}_R e^{j\delta}\right] = \frac{1}{2}\,[\boldsymbol{Y}_{SR}]\,\left[\boldsymbol{V}_S + \boldsymbol{V}_R e^{j\delta}\right] \tag{17}$$

The unknown variables in (17) are $\boldsymbol{Y}_{SR}$ and δ. It is well-known that the angle of diagonal elements of $\boldsymbol{Y}_{SR}$ equals 90°, while that of off-diagonal elements of $\boldsymbol{Y}_{SR}$ equals −90°. If the line is transposed, e.g., first row in (17) is written as:

$$\begin{aligned} &2\,\left(I_{S,a1} + I_{R,\,a1}e^{j\delta}\right) = y_s\,\left(V_{S,a1} + V_{R,a1}e^{j\delta}\right) \\ &+ y_{m1}\left(V_{S,b1} + V_{R,b1}e^{j\delta}\right) \\ &y_m\left(V_{S,b1} + V_{R,b1}e^{j\delta} + V_{S,c1} + V_{R,c1}e^{j\delta}\right) \end{aligned}$$

$$+ y'_{m12}\left(V_{S,a2} + V_{R,a2}e^{j\delta} + V_{S,b2} + V_{R,b2}e^{j\delta} + V_{S,c2} + V_{R,c2}e^{j\delta}\right) \tag{18}$$

where y_s, y_m, and y'_{m12} are the self-admittance for each phase, the mutual coupling shunt admittance between phases of the same circuit, and the mutual coupling shunt admittance between both circuits, respectively. In healthy conditions, the system is considered balanced 3-phase system, and hence:

$$V_{S,a2}+V_{R,a2}e^{j\delta}+V_{S,b2}+V_{R,b2}e^{j\delta}+V_{S,c2}+V_{R,c2}\ e^{j\delta} = 0 \tag{19}$$

$$V_{S,b1}+V_{R,b1}e^{j\delta}+V_{S,c1}+V_{R,c1}\ e^{j\delta} = -\left(V_{S,a1}+V_{R,a1}e^{j\delta}\right) \tag{20}$$

Accordingly, (18) can be written as:

$$(y_s - y_m) = 2(I_{S,a1} + I_{R,\ a1}e^{j\delta})/\left(V_{S,a1} + V_{R,a1}e^{j\delta}\right) \tag{21}$$

It can be noted that the angle of $(y_s - y_m)$ is equal to 90° since the angle of y_S equals 90°, while the angle of y_m equals −90°. The same equations can be obtained for the other phases of the line $(S - R)$. Hence, (17) is rewritten:

$$2\begin{bmatrix}\left(I_{S,a1} + I_{R,\ a1}e^{j\delta}\right)/\left(V_{S,a1} + V_{R,a1}e^{j\delta}\right)\\ \left(I_{S,b1} + I_{R,\ b1}e^{j\delta}\right)/\left(V_{S,b1} + V_{R,b1}e^{j\delta}\right)\\ \left(I_{S,c1} + I_{R,\ c1}e^{j\delta}\right)/\left(V_{S,c1} + V_{R,c1}e^{j\delta}\right)\\ \left(I_{S,a2} + I_{R,\ a2}e^{j\delta}\right)/\left(V_{S,a2} + V_{R,a2}e^{j\delta}\right)\\ \left(I_{S,b2} + I_{R,\ b2}e^{j\delta}\right)/\left(V_{S,b2} + V_{R,b2}e^{j\delta}\right)\\ \left(I_{S,c2} + I_{R,\ c2}e^{j\delta}\right)/\left(V_{S,c2} + V_{R,c2}e^{j\delta}\right)\end{bmatrix} = \begin{bmatrix}y_s - y_m\\ y_s - y_m\\ y_s - y_m\\ y_s - y_m\\ y_s - y_m\\ y_s - y_m\end{bmatrix} \tag{22}$$

Taking the angle of both sides with considering that the currents and voltages of identical phases in the two circuits are equal, one of the two circuits is enough to estimate δ.

$$arg\left\{\begin{matrix}\left(I_{S,a1} + I_{R,\ a1}e^{j\delta}\right)/\left(V_{S,a1} + V_{R,a1}e^{j\delta}\right)\\ \left(I_{S,b1} + I_{R,\ b1}e^{j\delta}\right)/\left(V_{S,b1} + V_{R,b1}e^{j\delta}\right)\\ \left(I_{S,c1} + I_{R,\ c1}e^{j\delta}\right)/\left(V_{S,c1} + V_{R,c1}e^{j\delta}\right)\end{matrix}\right\} = \begin{bmatrix}90^\circ\\ 90^\circ\\ 90^\circ\end{bmatrix} \tag{23}$$

where arg(·) refers to the phase angle. The unknown variable in (23) is only δ, which is easily obtained by solving (23) using "fsolve" MATLAB function. The next step is to deduce the FL equation for identical inter-circuit faults. In Fig. 3, the relation between pre-fault voltages ($\mathbf{V}_\mathrm{S}$ and $\mathbf{V}_\mathrm{R}$) at both terminals can be represented as:

$$[\boldsymbol{V}_S]\,e^{j\delta} - [\boldsymbol{V}_R] = [\boldsymbol{Z}_{SR}]\ \left([\boldsymbol{I}_S]\,e^{j\delta} - 0.5\times[\boldsymbol{Y}_{SR}]\,[\boldsymbol{V}_S]\,e^{j\delta}\right) \tag{24}$$

Besides, the pre-fault voltages at the FL ($\boldsymbol{V}_{F-pre}$) is written as a function of D_F and unsynchronized data at both terminals:

$$[\boldsymbol{V}_{F-pre}] = [\boldsymbol{V}_S]\ e^{j\delta} - D_F\,[\boldsymbol{Z}_{SR}]\,e^{j\delta}\,([\boldsymbol{I}_S] - 0.5\,[\boldsymbol{Y}_{SR}]\,[\boldsymbol{V}_S]) \tag{25}$$

$$[\boldsymbol{V}_{F-pre}] = [\boldsymbol{V}_R] - (1 - D_F)\,[\boldsymbol{Z}_{SR}]\,([\boldsymbol{I}_R] - 0.5\,[\boldsymbol{Y}_{SR}]\,[\boldsymbol{V}_R]) \tag{26}$$

Substituting (26) into (25):

$$([\boldsymbol{V}_S]\,e^{j\delta} - [\boldsymbol{V}_R]) = [\boldsymbol{Z}_{SR}]\ \left\{\left(D_F\,[\boldsymbol{I}_S]\,e^{j\delta} - (1 - D_F)\,[\boldsymbol{I}_R]\right) - 0.5\,[\boldsymbol{Y}_{SR}]\left(D_F\,[\boldsymbol{V}_S]\,e^{j\delta} - (1 - D_F)\,[\boldsymbol{V}_R]\right)\right\} \tag{27}$$

Taking the transpose of (27):

$$\left([\boldsymbol{V}_S]^T e^{j\delta} - [\boldsymbol{V}_R]^T\right) = \left\{D_F[\boldsymbol{I}_S]^T e^{j\delta} - (1 - D_F)\,[\boldsymbol{I}_R]^T - 0.5\left(D_F[\boldsymbol{V}_S]^T e^{j\delta} - (1 - D_F)\,[\boldsymbol{V}_R]^T\right)[\boldsymbol{Y}_{SR}]\right\}\ [\boldsymbol{Z}_{SR}] \tag{28}$$

For a generic fault on line $(S - R)$ in Fig. 2, the same steps are repeated after fault occurrence. Substituting (16) into (15):

$$([\boldsymbol{V}_{SF}]\ e^{j\delta_F} - [\boldsymbol{V}_{RF}]) = [\boldsymbol{Z}_{SR}]\ \left\{\left(D_F\,[\boldsymbol{I}_{SF}]\,e^{j\delta_F} - (1 - D_F)\,[\boldsymbol{I}_{RF}]\right) - 0.5\,[\boldsymbol{Y}_{SR}]\left({D_F}^2\,[\boldsymbol{V}_{SF}]\,e^{j\delta_F} - (1 - D_F)^2\,[\boldsymbol{V}_{RF}]\right)\right\} \tag{29}$$

where δ_F is the post-fault SA. Taking the transpose of (29):

$$\left([\boldsymbol{V}_{SF}]^T e^{j\delta_F} - [\boldsymbol{V}_{RF}]^T\right) = \left\{D_F[\boldsymbol{I}_{SF}]^T e^{j\delta_F} - (1 - D_F)\,[\boldsymbol{I}_{RF}]^T - 0.5\left({D_F}^2[\boldsymbol{V}_{SF}]^T e^{j\delta_F} - (1 - D_F)^2[\boldsymbol{V}_{RF}]^T\right)[\boldsymbol{Y}_{SR}]\right\}\ [\boldsymbol{Z}_{SR}] \tag{30}$$

Subtracting (30) from (28):

$$\left(\left[\boldsymbol{V}_S e^{j\delta} - \boldsymbol{V}_{SF}e^{j\delta_F}\right]^T - [\boldsymbol{V}_R - \boldsymbol{V}_{RF}]^T\right) = \left\{D_F\left[\boldsymbol{I}_S e^{j\delta} - \boldsymbol{I}_{SF}e^{j\delta_F}\right]^T - (1 - D_F)\,[\boldsymbol{I}_R - \boldsymbol{I}_{RF}]^T - 0.5\left(D_F\left(e^{j\delta}[\boldsymbol{V}_S]^T - D_F[\boldsymbol{V}_{SF}]^T e^{j\delta_F}\right) - (1 - D_F)\left([\boldsymbol{V}_R]^T - (1 - D_F)\,[\boldsymbol{V}_{RF}]^T\right)\right)[\boldsymbol{Y}_{SR}]\right\}\ [\boldsymbol{Z}_{SR}] \tag{31}$$

Multiplying both sides of (31) with $([\boldsymbol{I}_S]e^{j\delta} - 0.5[\boldsymbol{Y}_{SR}][\boldsymbol{V}_S]e^{j\delta})$ and substituting (24) into (31):

$$\left(\left[\boldsymbol{V}_S e^{j\delta} - \boldsymbol{V}_{SF}e^{j\delta_F}\right]^T - [\boldsymbol{V}_R - \boldsymbol{V}_{RF}]^T\right)\left([\boldsymbol{I}_S]\,e^{j\delta} - 0.5\,[\boldsymbol{Y}_{SR}]\,[\boldsymbol{V}_S]\,e^{j\delta}\right) = \left\{D_F\left[\boldsymbol{I}_S e^{j\delta} - \boldsymbol{I}_{SF}e^{j\delta_F}\right]^T - (1 - D_F)\,[\boldsymbol{I}_R - \boldsymbol{I}_{RF}]^T - 0.5\left(D_F\left([\boldsymbol{V}_S]^T e^{j\delta} - D_F[\boldsymbol{V}_{SF}]^T e^{j\delta_F}\right) - (1 - D_F)\left([\boldsymbol{V}_R]^T - (1 - D_F)\,[\boldsymbol{V}_{RF}]^T\right)\right)[\boldsymbol{Y}_{SR}]\right\}\left([\boldsymbol{V}_S]\,e^{j\delta} - [\boldsymbol{V}_R]\right) \tag{32}$$

The unknown variables in (32) are D_F and δ_F because δ is obtained utilizing pre-fault current and voltage data. Equation (32) is solved using the "fsolve" MATLAB function, where two solutions are obtained. The correct solution is that achieving $\mathrm{D_F}$

falls within 0 and 1 per-unit. Besides, to obtain $\boldsymbol{Y}_{SR}$, referring to (17) and ignoring mutual-admittance between different phases, the self-admittance of each phase is estimated utilizing pre-fault data:

$$\begin{bmatrix} y_{a1,a1} \\ y_{b1,b1} \\ y_{c1,c1} \\ y_{a2,a2} \\ y_{b2,b2} \\ y_{c2,c2} \end{bmatrix} = 2 \begin{bmatrix} \left(I_{S,a1} + I_{R,\,a1} e^{j\delta}\right) / \left(V_{S,a1} + V_{R,a1} e^{j\delta}\right) \\ \left(I_{S,b1} + I_{R,\,b1} e^{j\delta}\right) / \left(V_{S,b1} + V_{R,b1} e^{j\delta}\right) \\ \left(I_{S,c1} + I_{R,\,c1} e^{j\delta}\right) / \left(V_{S,c1} + V_{R,c1} e^{j\delta}\right) \\ \left(I_{S,a2} + I_{R,\,a2} e^{j\delta}\right) / \left(V_{S,a2} + V_{R,a2} e^{j\delta}\right) \\ \left(I_{S,b2} + I_{R,\,b2} e^{j\delta}\right) / \left(V_{S,b2} + V_{R,b2} e^{j\delta}\right) \\ \left(I_{S,c2} + I_{R,\,c2} e^{j\delta}\right) / \left(V_{S,c2} + V_{R,c2} e^{j\delta}\right) \end{bmatrix} \tag{33}$$

After calculating $\boldsymbol{Y}_{SR}$ and substituting into (32), it is clear that (32) does not rely on the line parameters. Besides, it is appropriate to utilize (32) for cases, where (15) fail to estimate the FL because (15) is more accurate, while (32) ignores the mutual-capacitance between different phases. In other words, (32) is applied when identical inter-circuit faults occur. Thus, a strategy is provided to determine when to apply both equations. For identical inter-circuit faults, the currents at line terminals of identical phases in the two circuits are equal ($\boldsymbol{I}_{SF1} = \boldsymbol{I}_{SF2}$ & $\boldsymbol{I}_{RF1} = \boldsymbol{I}_{RF2}$). Thus, $|\Delta \boldsymbol{I}_{SF}|$ and $|\Delta \boldsymbol{I}_{RF}|$ in (34) are theoretically zero for identical inter-circuit faults. However, to consider the errors in the CT measurements, typical CTs have protection classes of $5P20$ or $5P30$. Accordingly, the maximum CT error is $\pm 5\%$, as outlined in IEC 61869-2 [34]. Thus, a threshold value is set at 10% of the pre-fault current to consider the errors in CT measurements. If any value of $|\Delta \boldsymbol{I}_{SF}|$ or $|\Delta \boldsymbol{I}_{RF}|$ exceeds the threshold value, (15) is applied to estimate the FL.

$$|\Delta \boldsymbol{I}_{SF}| = |\boldsymbol{I}_{SF1} - \boldsymbol{I}_{SF2}| \ \& \ |\Delta \boldsymbol{I}_{RF}| = |\boldsymbol{I}_{RF1} - \boldsymbol{I}_{RF2}| \tag{34}$$

It is worth noting that the contributions of the proposed approach presented in this subsection compared to [14], are as follows:

- The developed FL method introduces a new approach to obtain the pre-fault SA using pre-fault data, as shown in (23). This can serve additional purposes beyond estimating the FL. Consequently, the self-admittance is computed using (33). This aspect is not addressed in [14], which does not allow estimating the pre-fault SA and line admittance using pre-fault data.
- Synchronism mismatches in the pre-fault and post-fault data may occur, as described in [26]. The developed FL method addresses this synchronism mismatch in the pre- and post-fault data. In contrast, the approach in [14] ignores this synchronism mismatch in the pre- and post-fault data, assuming that the SA remains the same for both the pre- and post-fault conditions.

A flow chart is provided in Fig. 4 to summarize the steps of the developed method. Once the fault is detected, $|\Delta \boldsymbol{I}_{SF}|$ and $|\Delta \boldsymbol{I}_{RF}|$ are calculated using (34). If maximum of $|\Delta \boldsymbol{I}_{SF}|$ and $|\Delta \boldsymbol{I}_{RF}|$ exceeds 0.1 pu, (15) is applied to calculate the FL. In contrast, if $|\Delta \boldsymbol{I}_{SF}|$ and $|\Delta \boldsymbol{I}_{RF}|$ are less than 0.1 pu, δ and fault distance is obtained using (23) and (32), respectively.

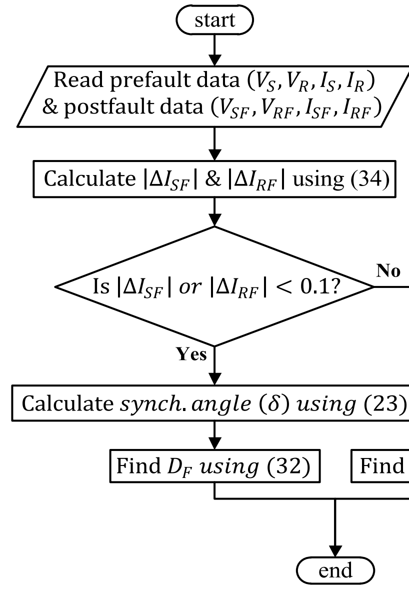

Fig. 4. Steps of the proposed FL method.

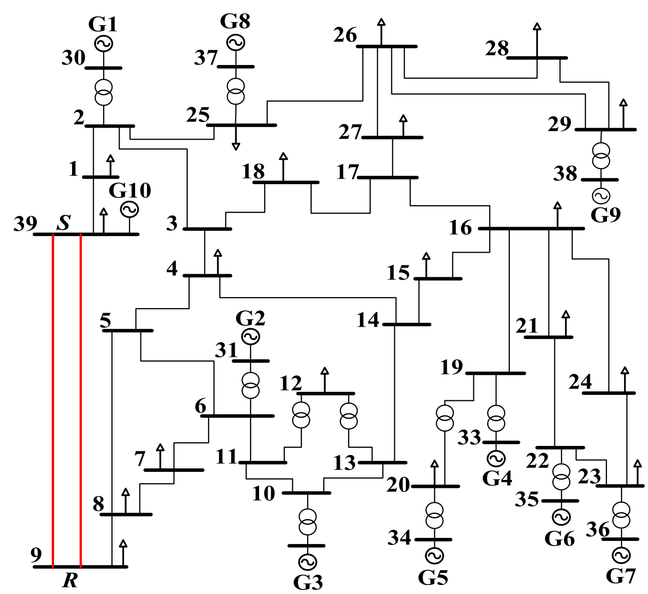

Fig. 5. Modified IEEE 39-bus system.

III. Simulation Results

The modified IEEE 39-bus system (230 kV, 60 Hz) in Fig. 5 is emulated on PSCAD/EMTDC, where its information is given in [32]. MATLAB is employed to execute all calculations. The 300 km double-circuit line is connected between buses 9 and 39. The line is emulated as an untransposed line using the frequency-dependent model to consider worst case. The information of CTs and VTs are given in Appendix. The measurements are

TABLE I
RESULTS OF ESTIMATED SA (δ) FOR DIFFERENT LINE LENGTHS

Delay (ms)	Actual δ	Error in Estimated SA ($\Delta\delta$)			
		300 km	250 km	200 km	150 km
1.3889	30º	0.113º	0.370º	0.559º	0.748º
2.7778	60º	0.113º	0.370º	0.559º	0.748º
4.1667	90º	0.113º	0.370º	0.559º	0.748º
5.5556	120º	0.113º	0.370º	0.559º	0.748º
6.9444	150º	0.113º	0.370º	0.559º	0.748º
8.3333	180º	0.113º	0.370º	0.559º	0.748º

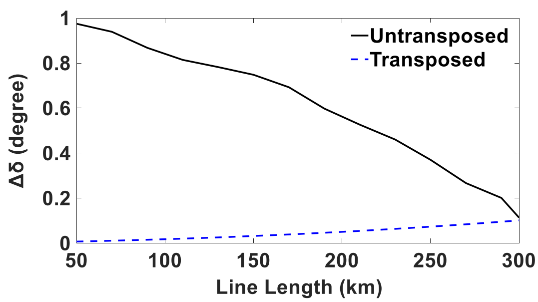

Fig. 6. Errors in the estimated SA ($\Delta\delta$) for different line lengths.

TABLE II
RESULTS OF ESTIMATED LINE ADMITTANCE FOR DIFFERENT LINE LENGTHS

Self-Admittance	Actual Value	Self-Admittance $\times 10^{-3}\ \Omega/km$		
		300 km	200 km	100 km
$y_{a1,a1}$	0.00364	0.00395	0.00399	0.00412
$y_{b1,b1}$	0.00380	0.00443	0.00448	0.00462
$y_{c1,c1}$	0.00361	0.00391	0.00395	0.00408
$y_{a2,a2}$	0.00364	0.00395	0.00399	0.00412
$y_{b2,b2}$	0.00380	0.00443	0.00448	0.00462
$y_{c2,c2}$	0.00361	0.00391	0.00395	0.00408
Transposed Line				
y_s	0.00360	0. 00401	0. 00399	0. 00397

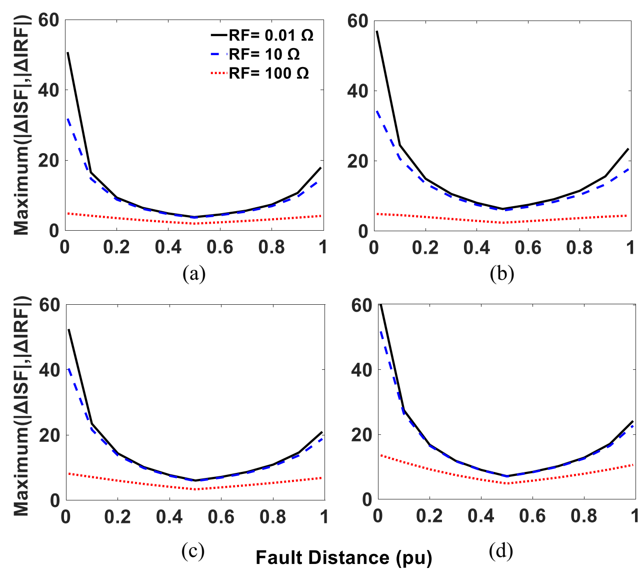

Fig. 7. Maximum of ($|\Delta I_{SF}|$, $|\Delta I_{RF}|$) per-unit for normal-shunt faults. (a) SLG. (b) LLG. (c) LL. (d) LLL.

sampled at 1.2 kHz, and one-cycle pre-fault and on-cycle post-fault measurements are employed to calculate the 60 Hz phasors using discrete Fourier transform. Consequently, it is assumed that the fault clearing time, including the operating time of the protective relay and the opening time of the circuit breaker, does not exceed 80 msec. The FL precision is assessed by estimating the FL error as:

$$FL\ Error\% = \frac{|calculated\ length - actual\ length|}{line\ length} \times 100\% \tag{35}$$

A. Evaluation for Synchronization Angle (SA) Estimation

To evaluate the developed technique for estimating δ, different intentional delays are involved in pre-fault measurements at terminal R. As an example, a delay of 4.16667 ms is equivalent to an actual δ of 90° for 60 Hz system. The results are displayed in Table I for various δ and line lengths. The errors in the estimated SA ($\Delta\delta$) are constant for same line length because same pre-fault data in (23) are utilized in each case. Besides, $\Delta\delta$ increases with decreasing line length due to the shunt capacitance influence, where it is more significant with increasing line length. In other words, the inequality between current phasors at both terminals increases with increasing line length, leading to accurate estimation of δ. Fig. 6 shows $\Delta\delta$ for untransposed and transposed lines with different line lengths, where $\Delta\delta$ is limited to less than 1°. $\Delta\delta$ is relatively low in the case of the transposed line compared to the untransposed line since the derivation in Section II-B assumes that the line is transposed. It is important to note that, according to IEEE standard [33], the expected time synchronization error in the measurements is ±0.57° (±26 μs for 60 Hz system). Thus, the estimated $\Delta\delta$ are still close to that stipulated by IEEE standard. The estimated SA is utilized in determining the FL in the next sections. Furthermore, the calculated self-admittance of each phase using (33) is provided in Table II for different line lengths. The errors in the estimated self-admittance are similar for both untransposed and transposed lines. Additionally, these errors increase gradually with decreasing line length since the errors in $\Delta\delta$ increase with decreasing line length, as explained earlier. However, the line admittance can be neglected for short lengths.

B. Normal-Shunt Faults

In normal-shunt faults in only one circuit, (15) is applied to obtain D_F since at least one element of $|\Delta \boldsymbol{I}_{SF}|$ and $|\Delta \boldsymbol{I}_{RF}|$ will exceed the threshold value of 0.1 pu. The line length, pre-fault SA, and post-fault SA are set at 300 km, 60°, and 120°, respectively. Fig. 7 shows the maximum of $|\Delta \boldsymbol{I}_{SF}|$ and $|\Delta \boldsymbol{I}_{RF}|$ for different normal-shunt faults (132 cases), including 1-line to

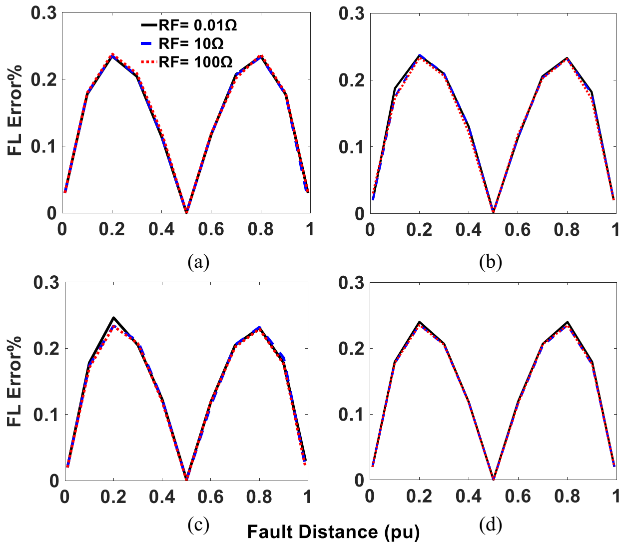

Fig. 8. FL error% for normal-shunt faults and various fault resistances. (a) SLG. (b) LLG. (c) LL. (d) LLL.

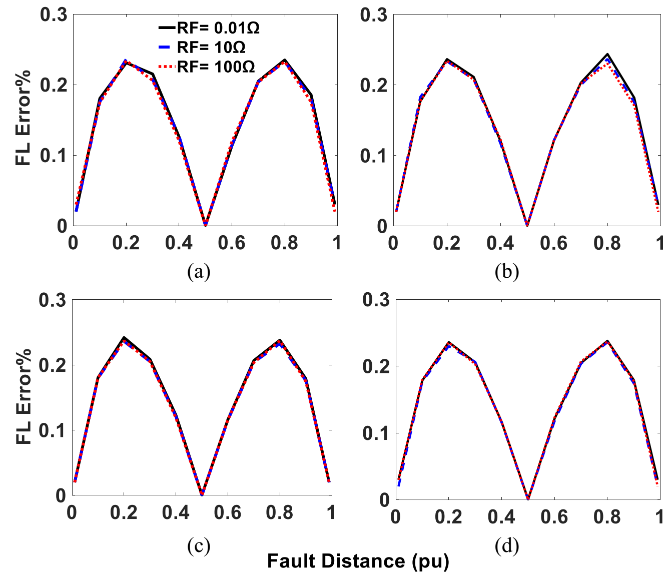

Fig. 9. FL error% for asymmetrical inter-circuit faults and fault resistances. (a) a1g-b2g. (b) a1-c2. (c) a1c1g-a2b2g. (d) b1c1-a2c2.

ground (SLG), 2-line to ground (LLG), 2-line (LL), and 3-line (LLL) faults. Different FLs (1% up to 99% of line length) and fault resistances (0.01, 10, and 100 Ω) are considered. As shown, the minimum of $|\Delta \boldsymbol{I}_{SF}|$ and $|\Delta \boldsymbol{I}_{RF}|$ is equal to 1.942 pu, which is much higher than the threshold value of 0.1 pu, and thus, (15) is applied. As displayed in Fig. 8, the maximum and average FL errors are equal to 0.246% and 0.138%, respectively. Besides, the FL error is zero at 50% of the line length for all cases because $|\Delta \boldsymbol{I}_{SF}|$ is always equal to $|\Delta \boldsymbol{I}_{RF}|$ when a fault occurs at 0.5 pu, as derived in Appendix C. Thus, substituting in (15), the estimated FL will always be 0.5 pu. Moreover, the FL error increases gradually when the FL moves away from the middle of the line because when a fault occurs near to line terminals, one side of the fault point is a short line, while other side is a long line. Therefore, one of the PI model utilized in (3) and (4) does not represent the long section of the line accurately. The developed method does not rely on fault resistance and type, and the outcomes assure its solid performance for normal-shunt faults.

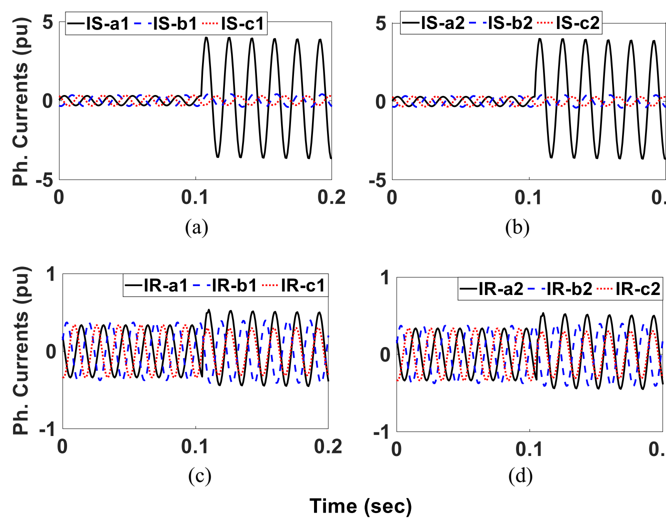

Fig. 10. Current waveforms of the double-circuit line at both terminals due to an identical inter-circuit fault ($a_1g - a_2g$): (a) Terminal S, circuit-1, (b) Terminal S, circuit-2, (c) Terminal R, circuit-1, and (d) Terminal R, circuit-2.

C. Inter-Circuit Faults in Different Phases in Both Circuits

For asymmetrical inter-circuit faults, (15) is applied to obtain D_F since at least two elements of $|\Delta \boldsymbol{I}_{SF}|$ and $|\Delta \boldsymbol{I}_{RF}|$ will exceed 0.1 pu. Different inter-circuit faults ($a_1g - b_2g$, a_1c_2, $a_1c_1g - a_2b_2g$, and $b_1c_1 - a_2c_2$) at different D_F and R_F are simulated. Due to limited space, the results for the maximum of $|\Delta \boldsymbol{I}_{SF}|$ and $|\Delta \boldsymbol{I}_{RF}|$ are not presented. However, similar results to those depicted in Fig. 7 are obtained. Notably, the minimum of $|\Delta \boldsymbol{I}_{SF}|$ and $|\Delta \boldsymbol{I}_{RF}|$ is equal to 2.323 pu, which is much higher than 0.1 pu. Thus, (15) is applied. In Fig. 9, the FL error% are provided for the simulated scenarios, where the maximum and average FL errors equal 0.244% and 0.139%, respectively. As observed, the developed method has a successful response for asymmetrical inter-circuit faults.

D. Inter-Circuit Faults in Identical Phases in Both Circuits

For identical inter-circuit faults involving identical phases in the two circuits, (15) fails in estimating D_F. Thus, (32) is applied to obtain D_F in such cases. It is expected that $|\Delta \boldsymbol{I}_{SF}|$ and $|\Delta \boldsymbol{I}_{RF}|$ will be zero since the currents of the same phases in both circuits will be theoretically identical at both terminals. Thus, it will be much less than 0.1 pu. Different identical inter-circuit faults ($a_1g - a_2g$, $a_1b_1g - a_2b_2g$, $a_1c_1 - a_2c_2$, and $a_1b_1c_1 - a_2b_2c_2$) are conducted with different D_F and R_F. Fig. 10 shows the phase currents for both circuits at each terminal due to an identical inter-circuit fault ($\mathrm{a_1g - a_2g}$) located at $\mathrm{D_F} = 0.1$ p.u. with $\mathrm{R_F} = 0.01\Omega$. Although the phase currents of both circuits are still equal at each terminal when the

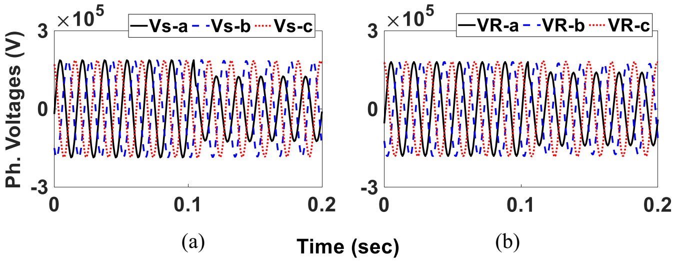

Fig. 11. Voltage waveforms of the double-circuit line at both terminals due to an identical inter-circuit fault ($a_1g - a_2g$): (a) Terminal S and (b) Terminal R.

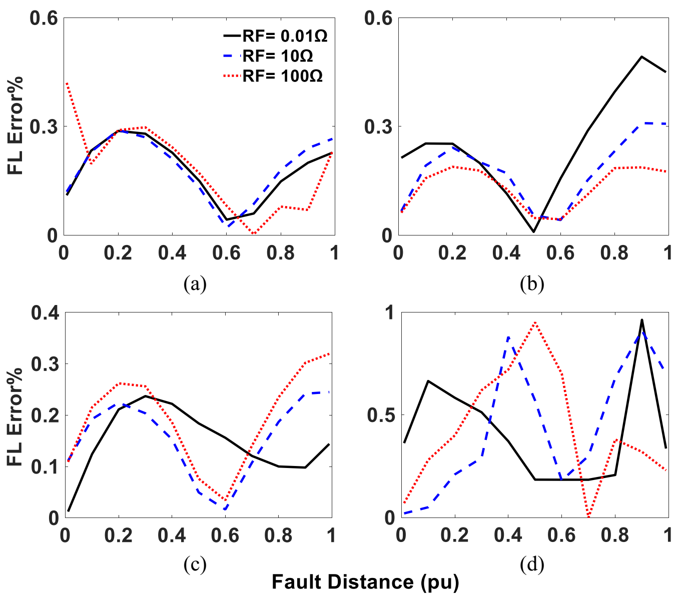

Fig. 12. FL error% for identical inter-circuit faults. (a) a1g-a2g. (b) a1b1g-a2b2g. (c) a1c1-a2c2. (d) a1b1c1-a2b2c2.

fault occurs, they increase. In addition, Fig. 11 shows the phase voltages for both circuits at each terminal, where the voltage of the faulted phases decreases at each terminal when the fault occurs. Moreover, the maximum of $|\Delta I_{SF}|$ and $|\Delta I_{RF}|$ is equal to 5.5496×10^{-12} pu, which is well below 0.1 pu. Thus, (32) is applied, and the FL errors are provided in Fig. 12. The maximum and average FL errors equal 0.963% and 0.241%, respectively. It is obvious that changing R_F has a minimal impact on the FL error, and the developed technique achieves a successful performance for all tested identical inter-circuit faults.

E. Influence of Measurement Errors

The VT maximum measurement error is typically $\pm3\%$ since their protection classes are $3P$ [35], while the CT maximum measurement error is typically $\pm5\%$ since their protection classes are $5P20$ or $5P30$ [34]. To consider VT and CT measurement errors, errors in voltage and current measurements are set at $+3\%$ and $+5\%$ at one terminal, respectively, while they are set at -3% and -5% at other terminal, respectively. Different fault types (c_1g, $a_1b_1c_1$, $a_1b_1 - b_2c_2$, and $b_1g - b_2g$) are conducted with different FLs (1% up to 99% of line length)

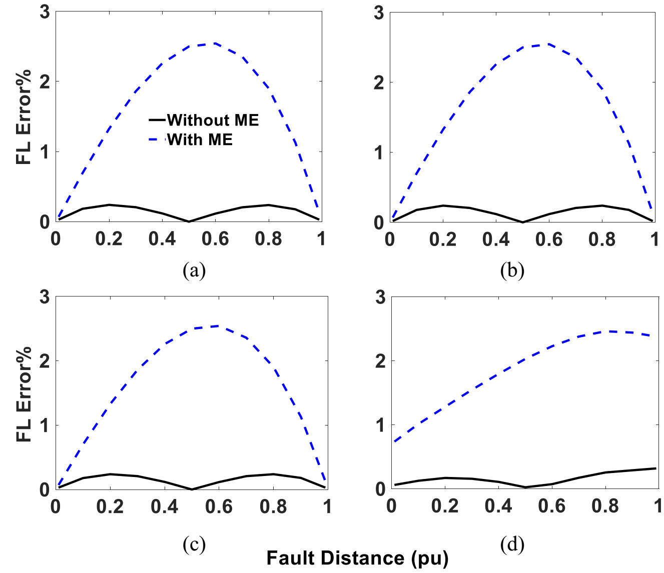

Fig. 13. FL error% considering measurement errors and line length of 300 km. (a) c1g. (b) a1b1c1. (c) a1b1-b2c2. (d) b1g-b2g.

and $R_F = 1\ \Omega$. Fig. 13 shows the FL errors with and without measurement errors. The maximum and average FL errors equal respectively 0.39% and 0.145% without measurement errors, while the maximum and average FL errors equal, respectively, 2.546% and 1.606% with measurement errors. The FL error is about 2.5% at $D_F = 0.5$ pu for the fault types (c_1g, $a_1b_1c_1$, and $a_1b_1 - b_2c_2$), where (15) is applied for estimating the FL. $|\Delta I_{SF}|$ is always equal to $|\Delta I_{RF}|$ when a fault occurs at 0.5 pu, as derived in Appendix C. However, as the measurement errors in the CTs are assumed to be $+5\%$ at one-end and -5% at other end, the estimated error is about 2.5%. The VT and CT measurement errors greatly affect the FL precision. However, in the context of the overhead lines, they are still within acceptable limits considering maximum measurement errors. Furthermore, the above scenarios are repeated considering a line length of 100 km. Fig. 14 shows the FL errors with and without measurement errors. The maximum and average FL errors equal, respectively, 0.111% and 0.840% without measurement errors, while the maximum and average FL errors equal respectively 2.499% and 1.655% with measurement errors. Notably, similar outcomes are achieved when compared to the results obtained for a line length of 300 km.

F. Testing of Evolving Faults

The evolving faults are ground faults that originate in one phase and propagate to another phase at the same fault point after a short duration [36]. To assess the impact of evolving faults on the developed FL method, simulations are conducted for various scenarios outlined in Table III, including different normal-shunt and inter-circuit ground faults, different FLs (10% up to 90% of line length), fault resistances, and fault inception angles. The maximum and average FL errors equal 0.24% and 0.163%, respectively. It is evident that the developed method can estimate accurately the locations of the evolving faults.

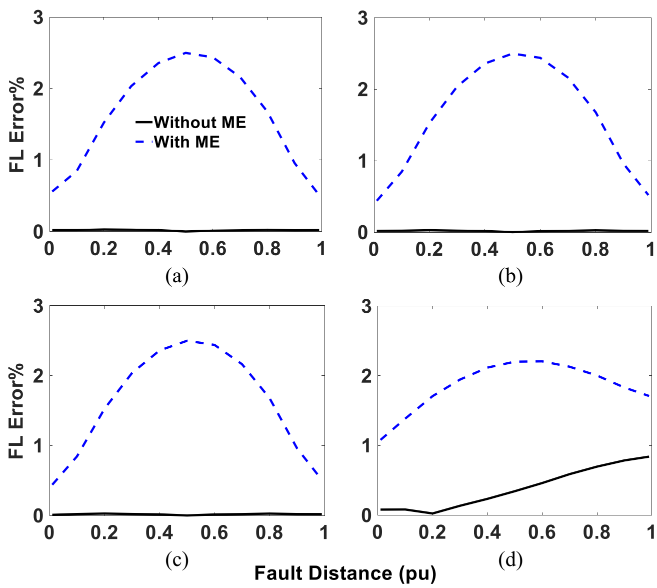

Fig. 14. FL error% considering measurement errors and line length of 100 km. (a) c1g. (b) a1b1c1. (c) a1b1-b2c2. (d) b1g-b2g.

TABLE III
RESULTS OF EVOLVING FAULTS

D_F (pu)	Fault Condition 1			Fault Condition 2			FL Error%
	Type	R_F (Ω)	δ_F°	Type	R_F (Ω)	δ_F°	
0.1	a_1g	0.1	0	b_1g	0.1	45	0.18
0.2	a_1g	50	0	c_1g	1	90	0.23
0.3	b_1g	5	0	c_1g	20	135	0.20
0.4	c_1g	100	0	a_2g	25	180	0.12
0.5	a_1g	10	45	b_2g	0.5	90	0.00
0.6	a_2g	0.01	45	b_1g	1	135	0.11
0.7	b_2g	0.1	45	c_1g	30	180	0.21
0.8	c_2g	80	90	a_1g	15	135	0.24
0.9	c_2g	0.5	90	b_1g	40	180	0.18

G. Testing of Different Loading Conditions

The FL accuracy may be influenced by the changes in the loading conditions. In order to emphasize the impact of different loading conditions, the developed FL method is evaluated with different values of pre-fault current (0.1, 0.5, and 1 pu). The FL results are outlined in Table IV considering all fault types and FLs (0.1, 0.5, and 0.9 pu). The results in Table IV demonstrate the robustness of the developed FL method against varying load conditions, where the maximum and average FL errors equal 0.20% and 0.123%, respectively. The results reveal the efficacy of the developed method for locating faults in double-circuit lines.

H. Testing of Only Single-Circuit Line

The previous FL methods in [28] and [31] are not applicable if one of the two circuits is out-of-service, while the developed FL method is applicable in such cases by solving (32). To verify the developed FL method under such conditions, various scenarios are implemented with different fault types, FLs (0.1, 0.5, and 0.9 pu), and fault resistances (0.01, 1, and 100 Ω). The FL results are outlined in Table V, where the maximum and average FL errors equal 0.76% and 0.17%, respectively. In the context of overhead lines, the FL errors remain within acceptable limits, and the results demonstrate the effectiveness of the developed method, even when one of the two circuits is out-of-service.

TABLE IV
RESULTS FOR DIFFERENT LOADING CONDITIONS

Pre-fault Current	D_F (pu)	FL Error%					
		c_1g	b_1c_1g	a_1c_1	$a_1b_1c_1$	b_1g-c_2g	c_1g-c_2g
$0.1\ pu$	0.1	0.18	0.17	0.18	0.18	0.17	0.11
	0.5	0.00	0.00	0.00	0.00	0.00	0.18
	0.9	0.18	0.18	0.18	0.18	0.18	0.18
$0.5\ pu$	0.1	0.18	0.18	0.17	0.18	0.18	0.11
	0.5	0.00	0.00	0.00	0.00	0.00	0.19
	0.9	0.18	0.18	0.18	0.18	0.18	0.12
$1\ pu$	0.1	0.18	0.17	0.17	0.18	0.18	0.12
	0.5	0.00	0.00	0.00	0.00	0.00	0.20
	0.9	0.18	0.18	0.18	0.18	0.18	0.08

TABLE V
RESULTS FOR DIFFERENT FAULT TYPES CONSIDERING SINGLE-CIRCUIT LINE

D_F (pu)	R_F (Ω)	FL Error%			
		SLG	LLG	LL	LLL
$0.1\ pu$	0.01	0.13	0.17	0.16	0.25
	1	0.08	0.17	0.15	0.26
	100	0.31	0.10	0.14	0.06
$0.5\ pu$	0.01	0.00	0.00	0.03	0.25
	1	0.07	0.00	0.03	0.19
	100	0.32	0.21	0.71	0.03
$0.9\ pu$	0.01	0.01	0.15	0.10	0.05
	1	0.09	0.16	0.11	0.14
	100	0.66	0.18	0.05	0.76

I. Influence of CT Saturation

The CT may be saturated, if a severe fault occurs. The burden impedance of the CT secondary side is one of the main factors causing the saturation of the CT. With increasing the CT burden impedance, the CT is likely to be saturated; especially in the case of double- and three-line faults due to the high possibility of the decaying DC component. To demonstrate the developed method against the CT saturation, the burden impedance is selected at 2.5 Ω, and a three-phase fault ($a_1b_1c_1$) is carried out near to one terminal, i.e., at 5% of the line length away from terminal (S) with a very low R_F of 0.01 Ω. Fig. 15 shows the current waveforms of the two circuits at the nearest terminal (S). The CTs of phases b_1 and c_1 of circuit-1 (I_{S-b1} and I_{S-c1}) saturates within 3 cycles after the fault instant, while the CTs of the healthy phases of circuit-2 do not saturate. In this case, (15) is applied to obtain the FL, and the FL error is estimated to be 0.53%.

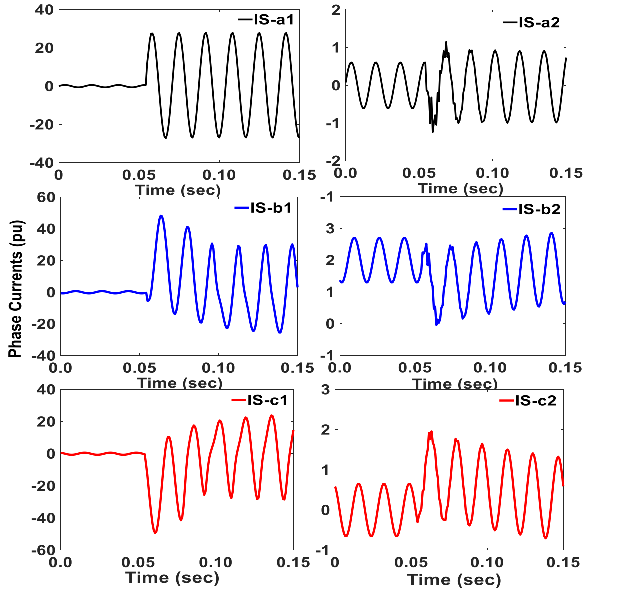

Fig. 15. Current waveforms of the double-circuit line at terminal S due to a three-line fault in circuit-1at 5% of line length away from terminal *S*.

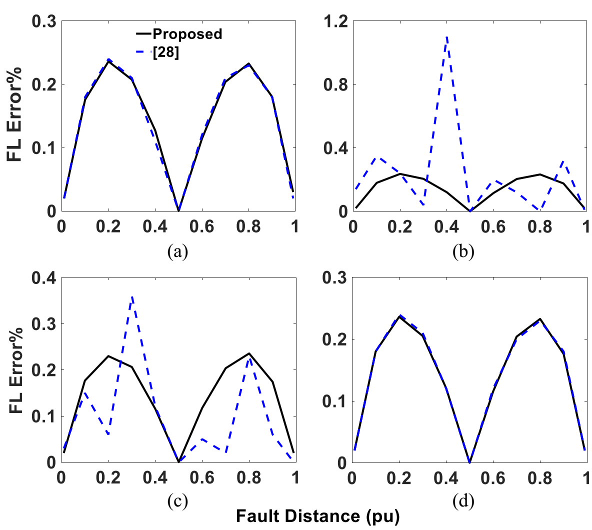

Fig. 16. FL error% for the developed method and [28] for different FLs and fault types. (a) SLG. (b) LL. (c) LLL. (d) a1c1g-a2b2g.

J. Comparative With Existing Techniques

In [26], the derived FL equation has two unknown variables (SA between both terminals and fault distance), and this method is not valid for identical inter-circuit faults. For the purpose of comparison, Different fault types are conducted, including normal-shunt faults and non-identical inter-circuit faults, with different FLs and $R_F = 1\,\Omega$. The FL errors are given in Fig. 16, where the maximum and average FL errors are respectively 0.24% and 0.14% for the developed method compared with 1.10% and 0.15% for that in [28]. The developed method is more accurate than that in [28] in the case of the non-ground faults because the FL in [28] is obtained in the sequence-domain, where positive, negative, or zero-sequence component can be utilized in the case of the untransposed lines. Conversely, the developed method is formulated in the phase-domain, combining all phases together as depicted in (15), which provide more accurate results.

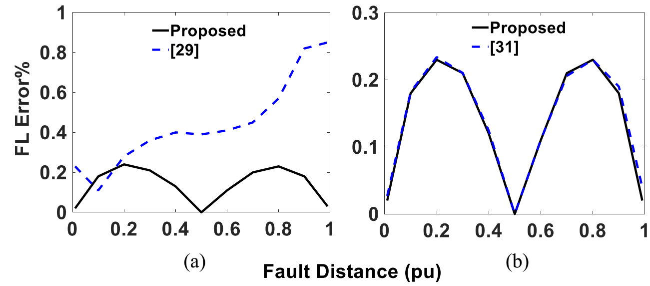

Fig. 17. FL error%: (a) Developed method and [29], (b) Developed method and [31]. (a) a1g-b2g. (b) a1-b2.

In [29], the FL method is introduced for double-circuit lines relying on unsynchronized positive-sequence current and voltage data without the need for line parameters and ignoring line capacitance. It relies on establishing a correlation between the unknown SA and fault point to estimate the FL. The FL equation is derived employing the lumped parameter line model with ignoring the line capacitance. Then, the least-square error approach is applied to estimate the FL utilizing unsynchronized data from both terminals. To compare the developed method with this technique, inter-circuit faults $(a_1g - b_2g)$ are conducted with different FLs and $R_F = 5\,\Omega$. As shown in Fig. 17(a), the maximum and average FL errors are respectively 0.24% and 0.14% for the developed method compared with 0.85% and 0.44% for that in [29]. It is evident that the developed method achieves better performance than that in [29].

Besides, the developed method is compared with the technique in [31]. This technique introduces a FL algorithm on a transposed double-circuit line without the need for line parameters and utilizing unsynchronized positive-sequence current and voltage data. It takes into account the distributed parameter line model in FL derivation. Inter-circuit faults $(a_1 - b_2)$ are conducted with different FLs and $R_F = 5\,\Omega$. As presented in Fig. 17(b), the maximum and average FL errors are respectively 0.230% and 0.137% for the developed method compared with 0.230% and 0.141% for that in [31]. While the proposed method relies on the π model, it attains similar results to those in [31], which relies on the distributed parameter line model. Additionally, the technique in [31] fails when an identical inter-circuit fault occurs, and if one of the two circuits is out-of-service.

Moreover, the developed method is compared with the techniques in [25] and [27], which are applicable for single-circuit lines. A SLG faults are conducted with different FLs and $R_F = 1\,\Omega$. As shown in Fig. 18, the maximum and average FL errors are respectively 0.155% and 0.08% for the developed method compared with 0.266% and 0.138% for that in [25], and 0.550% and 0.245% for that in [27]. It is clear that the developed method provides more accurate FL results compared with those in [25] and [27].

The proposed method is evaluated in comparison with existing techniques in the literature [28], [29], [30], [31], which are applied to the double-circuit lines, as illustrated in Table VI. All

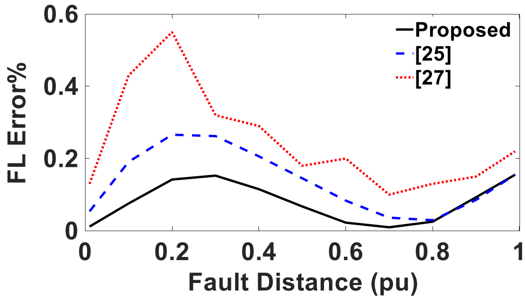

Fig. 18. FL error% for the developed method, [25], and [27].

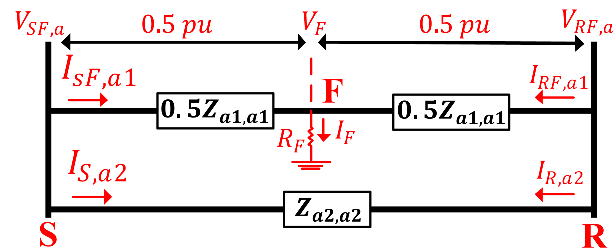

Fig. 19. Double-circuit line representation during fault conditions (lumped line model).

TABLE VI
COMPARISON WITH EXISTING TECHNIQUES

Item	FL Technique				
	[28]	[29]	[30]	[31]	Proposed
Number of Circuits	2	2	2	2	2
Fault Resistance	Yes	Yes	Yes	Yes	Yes
All Fault Type	No	No	Yes	No	Yes
Line Capacitance	Yes	No	Yes	Yes	Yes
Synchronism mismatch	N.A.	N.A.	No	N.A.	Yes
Different Loading Conditions	N.A.	N.A.	No	N.A.	Yes
Measurement Errors	Yes	No	No	No	Yes

*N.A.: Not Applicable

existing techniques and proposed method were tested against low and high fault resistances. Only the proposed method and [30] consider all fault types, including normal-shunt faults as well as identical and non-identical inter-circuit faults. In addition, all existing techniques and proposed method consider line capacitance in FL derivation, except [29]. Furthermore, the techniques in [28], [29], and [31] rely only on post-fault data. Thus, they are not affected by pre-fault loading conditions, and there is no need to calculate the pre-fault SA. On the other hand, the proposed method and [30] utilize pre- and post-fault data, which requires considering different loading conditions and calculating both pre- and post-fault SA. However, unlike the proposed method, the technique in [30] does not account for different loading conditions and different synchronism mismatches in the pre- and post-fault data. Finally, only the proposed method and [28] take into account the effect of measurement errors, unlike other techniques.

IV. CONCLUSION

A parameter-free FL method is introduced for the double-circuit transmission lines using the unsynchronized pre- and post-fault voltage and current data. Firstly, the FL equation is deduced for normal-shunt and non-identical inter-circuit faults, where it is based on equating the voltage phasors' difference at the FL between identical phases in the two circuits. The unsynchronized current phasors at both line terminals are only needed. However, the developed FL equation is viable for all fault types except the identical inter-circuit faults. Therefore, a FL equation is derived in the case of the identical inter-circuit faults without the need for line parameters. Besides, a time synchronization is not needed since a methodology is proposed to obtain the SA between both terminals utilizing the pre-fault data. The simulation results affirm the high efficiency of the developed method for several fault resistances, locations, and types. Besides, the developed method offers a solid performance for the inter-circuit faults, evolving faults, measurement errors, and different loading conditions. Furthermore, it remains applicable when one of the two circuits is out-of-service.

APPENDIX

A. Derivation of the Right-Hand Side of (10) and (11)

The derivation of right-hand side of (10) and (11) is shown in the top of the next page.

B. VT Main Information

Description	Value
Ratio	$230/0.1\ kV$
Capacitances	$134.952\ nF$ & $2.92\ nF$
Inductance for Compensation	$42\ H$
Series Impedance of the VT Burden	$301 + 904.78i\ \Omega$
Parallel Resistance of the VT Burden	785.1Ω

C. CT Main Information

PSCAD Model	Ratio	Impedance of the Burden
JA	$400/1A$	$0.50 + 0.30i\ \Omega$

D. Faults At 50% of Line Length

For simplicity, consider the lumped-line model and self-impedance of the double-circuit line only. Fig. 19 shows a (a_1g) fault at 0.5 per-unit in ciccuit-1 and corresponding phase a_2 in ciccuit-2, which are connected to same buses at line ends. The

$$[\boldsymbol{Z_{SR}}][\boldsymbol{I_{SF}}] = \begin{bmatrix} \boldsymbol{z_{a1,a1}I_{SF,a1}} + \boldsymbol{z_{a1,b1}I_{SF,b1}} + \boldsymbol{z_{a1,c1}I_{SF,c1}} + \boldsymbol{z_{a1,a2}I_{SF,a2}} + \boldsymbol{z_{a1,b2}I_{SF,b2}} + \boldsymbol{z_{a1,c2}I_{SF,c2}} \\ \boldsymbol{z_{b1,a1}I_{SF,a1}} + \boldsymbol{z_{b1,b1}I_{SF,b1}} + \boldsymbol{z_{b1,c1}I_{SF,c1}} + \boldsymbol{z_{b1,a2}I_{SF,a2}} + \boldsymbol{z_{b1,b2}I_{SF,b2}} + \boldsymbol{z_{b1,c2}I_{SF,c2}} \\ \boldsymbol{z_{c1,a1}I_{SF,a1}} + \boldsymbol{z_{c1,b1}I_{SF,b1}} + \boldsymbol{z_{c1,c1}I_{SF,c1}} + \boldsymbol{z_{c1,a2}I_{SF,a2}} + \boldsymbol{z_{c1,b2}I_{SF,b2}} + \boldsymbol{z_{c1,c2}I_{SF,c2}} \\ \boldsymbol{z_{a2,a1}I_{SF,a1}} + \boldsymbol{z_{a2,b1}I_{SF,b1}} + \boldsymbol{z_{a2,c1}I_{SF,c1}} + \boldsymbol{z_{a2,a2}I_{SF,a2}} + \boldsymbol{z_{a2,b2}I_{SF,b2}} + \boldsymbol{z_{a2,c2}I_{SF,c2}} \\ \boldsymbol{z_{b2,a1}I_{SF,a1}} + \boldsymbol{z_{b2,b1}I_{SF,b1}} + \boldsymbol{z_{b2,c1}I_{SF,c1}} + \boldsymbol{z_{b2,a2}I_{SF,a2}} + \boldsymbol{z_{b2,b2}I_{SF,b2}} + \boldsymbol{z_{b2,c2}I_{SF,c2}} \\ \boldsymbol{z_{c2,a1}I_{SF,a1}} + \boldsymbol{z_{c2,b1}I_{SF,b1}} + \boldsymbol{z_{c2,c1}I_{SF,c1}} + \boldsymbol{z_{c2,a2}I_{SF,a2}} + \boldsymbol{z_{c2,b2}I_{SF,b2}} + \boldsymbol{z_{c2,c2}I_{SF,c2}} \end{bmatrix} \quad \text{(A1)}$$

The same phases of both circuits in (A1) are subtracted from each other:

$$[\Delta(\boldsymbol{Z_{SR}I}_{SF})] = \begin{bmatrix} (z_{a1,a1}-z_{a1,a2})(I_{SF,a1}-I_{SF,a2})+(z_{a1,b1}-z_{b1,a2})(I_{SF,b1}-I_{SF,b2})+(z_{a1,c1}-z_{c1,a2})(I_{SF,c1}-I_{SF,c2}) \\ (z_{b1,a1}-z_{a1,b2})(I_{SF,a1}-I_{SF,a2})+(z_{b1,b1}-z_{b1,b2})(I_{SF,b1}-I_{SF,b2})+(z_{b1,c1}-z_{c1,b2})(I_{SF,c1}-I_{SF,c2}) \\ (z_{c1,a1}-z_{a1,c2})(I_{SF,a1}-I_{SF,a2})+(z_{c1,b1}-z_{b1,c2})(I_{SF,b1}-I_{SF,b2})+(z_{c1,c1}-z_{c1,c2})(I_{SF,c1}-I_{SF,c2}) \end{bmatrix} \quad \text{(A2)}$$

Rearrange:

$$[\Delta(\boldsymbol{Z_{SR}I}_{SF})] = \begin{bmatrix} z_{a1,a1}-z_{a1,a2} & z_{a1,b1}-z_{b1,a2} & z_{a1,c1}-z_{c1,a2} \\ z_{b1,a1}-z_{a1,b2} & z_{b1,b1}-z_{b1,b2} & z_{b1,c1}-z_{c1,b2} \\ z_{c1,a1}-z_{a1,c2} & z_{c1,b1}-z_{b1,c2} & z_{c1,c1}-z_{c1,c2} \end{bmatrix} \begin{bmatrix} I_{SF,a1}-I_{SF,a2} \\ I_{SF,b1}-I_{SF,b2} \\ I_{SF,c1}-I_{SF,c2} \end{bmatrix} \quad \text{(A3)}$$

Similarly:

$$[\Delta(\boldsymbol{Z_{SR}I}_{RF})] = \begin{bmatrix} z_{a1,a1}-z_{a1,a2} & z_{a1,b1}-z_{b1,a2} & z_{a1,c1}-z_{c1,a2} \\ z_{b1,a1}-z_{a1,b2} & z_{b1,b1}-z_{b1,b2} & z_{b1,c1}-z_{c1,b2} \\ z_{c1,a1}-z_{a1,c2} & z_{c1,b1}-z_{b1,c2} & z_{c1,c1}-z_{c1,c2} \end{bmatrix} \begin{bmatrix} I_{RF,a1}-I_{RF,a2} \\ I_{RF,b1}-I_{RF,b2} \\ I_{RF,c1}-I_{RF,c2} \end{bmatrix} \quad \text{(A4)}$$

voltages at both terminals are written as:

$$V_{SF}, a = 0.5Z_{a1,a1}I_{SF,a1} + I_F R_F \quad \text{(C1)}$$

$$V_{RF}, a = 0.5Z_{a1,a1}I_{RF,a1} + I_F R_F \quad \text{(C2)}$$

$$V_{SF}, a - V_{RF}, a = Z_{a2,a2}\, I_{S,a2} \quad \text{(C3)}$$

$$I_{S,a2} = -I_{R,a2} \,\&\, Z_{a2,a2} = Z_{a1,a1} \quad \text{(C4)}$$

where I_F is the ground fault current, substituting (C1) and (C2) into (C3):

$$0.5Z_{a1,a1}\,(I_{SF,a1} - I_{RF,a1}) = Z_{a2,a2}\, I_{S,a2} \quad \text{(C5)}$$

Considering (C4), rearranging (C5):

$$(I_{SF,a1} - I_{S,a2}) = (I_{RF,a1} - I_{R,a2}) \quad \text{(C6)}$$

It is clear that when a fault occurs at 0.5 per-unit, the difference between the phase currents of both circuits at one terminal is equal to that of the other terminal. The same derivation can be also carried out for other fault types.

References

[1] M. M. Saha, J. J. Izykowski, and E. Rosolowski, *Fault Location on Power Networks*, 1st ed. London, U.K.: Springer, 2010.

[2] R. Liang et al., “Fault location method in power network by applying accurate information of arrival time differences of modal traveling waves,” *IEEE Trans. Ind. Informat.*, vol. 16, no. 5, pp. 3124–3132, May 2020..

[3] F. V. Lopes, K. M. Dantas, K. M. Silva, and F. B. Costa, “Accurate two-terminal transmission line fault location using traveling waves,” *IEEE Trans. Power Del.*, vol. 33, no. 2, pp. 873–880, Apr. 2018.

[4] J. -A. Jiang et al., “A hybrid framework for fault detection, classification, and location-part I: Concept, structure, and methodology,” *IEEE Trans. Power Del.*, vol. 26, no. 3, pp. 1988–1998, Jul. 2011.

[5] J. -A. Jiang et al., “A hybrid framework for fault detection, classification, and location-part II: Implementation and test results,” *IEEE Trans. Power Del.*, vol. 26, no. 3, pp. 1999–2008, Jul. 2011.

[6] D. Lu et al., “Time-domain transmission line fault location method with full consideration of distributed parameters and line asymmetry,” *IEEE Trans. Power Del.*, vol. 35, no. 6, pp. 2651–2662, Dec. 2020.

[7] A. Saber, H. H. Zeineldin, T. H. El-Fouly, and A. Al-Durra, “Time-domain fault location algorithm for double-circuit transmission lines connected to large scale wind farms,” *IEEE Access*, vol. 9, pp. 11393–11404, 2021.

[8] L. Ji, X. Tao, Y. Fu, Y. Fu, Y. Mi, and Z. Li, “A new single ended fault location method for transmission line based on positive sequence superimposed network during auto-reclosing,” *IEEE Trans. Power Del.*, vol. 34, no. 3, pp. 1019–1029, Jun. 2019.

[9] A. Saber, H. H. Zeineldin, T. H. El-Fouly, and A. Al-Durra, “A new fault location scheme for parallel transmission lines using one-terminal data,” *Int. J. Elect. Power Energy Syst.*, vol. 135, Feb. 2022, Art. no. 107548.

[10] Y. Liu, B. Wang, X. Zheng, D. Lu, M. Fu, and N. Tai, “Fault location algorithm for non- homogeneous transmission lines considering line asymmetry,” *IEEE Trans. Power Del.*, vol. 35, no. 5, pp. 2425–2437, Oct. 2020.

[11] J. Izykowski et al., “Accurate noniterative fault-location algorithm utilizing two-end unsynchronized measurements,” *IEEE Trans. Power Del.*, vol. 25, no. 1, pp. 72–80, Jan. 2010.

[12] A. Saber, “New fault location algorithm for four-circuit overhead lines using unsynchronized current measurements,” *Int. J. Elect. Power Energy Syst.*, vol. 120, Sep. 2020, Art. no. 106037.

[13] Y. Liao and N. Kang, “Fault-location algorithms without utilizing line parameters based on the distributed parameter line model,” *IEEE Trans. Power Del.*, vol. 24, no. 2, pp. 579–584, Apr. 2009.

[14] C. A. Apostoloppulos and G. N. Korres, “A novel algorithm for locating faults on transposed/untransposed transmission lines without utilizing line parameters,” *IEEE Trans. Power Del.*, vol. 25, no. 4, pp. 2328–2338, Oct. 2010.

[15] G. Preston, Z. Radojevic, C. H. Kim, and V. Terzija, “New settings-free fault location algorithm based on synchronised sampling,” *IET Gener., Transmiss. Distrib.*, vol. 5, no. 3, pp. 376–383, Mar. 2011.

[16] V. Terzija, Z. M. Radojevic, and G. Preston, “Flexible synchronized measurement technology-based fault locator,” *IEEE Trans. Smart Grid*, vol. 6, no. 2, pp. 866–873, Mar. 2015.

[17] M. Popov, S. Parmar, G. Rietveld, G. Preston, Z. Radojevic, and V. Terzija, “Methodology for testing a parameter-free fault locator for transmission lines,” *Elect. Power Syst. Res.*, vol. 138, pp. 92–98, 2016.

[18] M. Davoudi, J. Sadeh, and E. Kamyab, “Parameter-free fault location for transmission lines based on optimisation,” *IET Gener., Transmiss. Distrib.*, vol. 9, no. 11, pp. 1061–1068, Aug. 2015.

[19] M. Davoudi, J. Sadeh, and E. Kamyab, “Transient-based fault location on three-terminal and tapped transmission lines not requiring line parameters,” *IEEE Trans. Power Del.*, vol. 33, no. 1, pp. 179–188, Feb. 2018.

[20] A. S. Dobakhshari, “Noniterative parameter-free fault location on untransposed single-circuit transmission lines,” *IEEE Trans. Power Del.*, vol. 28, no. 3, pp. 1636–1644, Jun. 2017.

[21] D. Lu, Y. Liu, S. Chen, B. Wang, and D. Lu, “An improved noniterative parameter-free fault location method on untransposed transmission lines using multi-section models,” *IEEE Trans. Power Del.*, vol. 37, no. 3, pp. 1356–1369, Jun. 2022.

[22] S. M. Hashemian, S. N. Hashemian, and M. Gholipour, “Unsynchronized parameter free fault location scheme for hybrid transmission line,” *Electr. Power Syst. Res.*, vol. 192, Jan. 2021, Art. no. 106982.

[23] O. D. Naidu, S. Zubic, A. V. S. S. R. Sai, A. N. Praveen, P. Cost, and H. Eriksson, “Economical setting-free double-ended fault locator for transmission lines: Experiences from recent pilot installations,” *IEEE Access*, vol. 10, pp. 96805–96820, 2022.

[24] D. Lu, Y. Liu, D. Lu, B. Wang, and X. Zheng, “Unsynchronized fault location on untransposed transmission lines with fully distributed parameter model considering line parameter uncertainties,” *Elect. Power Syst. Res.*, vol. 202, Jan. 2022, Art. no. 107622.

[25] K. Kalita, S. Anand, and S. Parida, “A closed form solution for line parameter-less fault location with unsynchronized measurements,” *IEEE Trans. Power Del.*, vol. 37, no. 3, pp. 1997–2006, Jun. 2022.

[26] K. Kalita, S. Anand, and S. K. Parida, “An improved parameter-free fault locator for untransposed line with unsynchronized terminals,” *IEEE Trans. Power Del.*, vol. 37, no. 6, pp. 5480–5483, Dec. 2022.

[27] K. Kalita, S. Anand, and S. K. Parida, “An enhanced parameter-free fault locator for untransposed line with unsynchronized terminals,” *IEEE Trans. Power Del.*, vol. 38, no. 5, pp. 3733–3736, Oct. 2023.

[28] C. A. Apostoloppulos and G. N. Korres, “A novel fault-location algorithm for double-circuit transmission lines without utilizing line parameters,” *IEEE Trans. Power Del.*, vol. 26, no. 3, pp. 1467–1478, Jul. 2011.

[29] N. I. Elkalashy, T. A. Kawady, W. M. Khater, and A. I. Taalab, “Unsynchronized fault-location technique for double-circuit transmission systems independent of line parameters,” *IEEE Trans. Power Del.*, vol. 31, no. 4, pp. 1591–1600, Aug. 2016.

[30] B. Wang, Y. Liu, D. Lu, K. Yue, and Y. Nie, “Unsynchronized parameter-free fault location for two or three terminal double-circuit transmission lines sharing the same tower via unscented Kalman filter,” *IEEE Trans. Power Del.*, vol. 38, no. 3, pp. 1731–1746, Jun. 2023.

[31] K. Kalita, S. Anand, and S. K. Parida, “Distributed parameter based setting-free fault locator for double-circuit line using fault data,” *IEEE Trans. Power Del.*, vol. 38, no. 4, pp. 2981–2984, Aug. 2023.

[32] IEEE 39 Bus System, 2022. [Online]. Available: https://www.pscad.com/knowledge-base/article/28

[33] *Measuring Relays and Protection Equipment - Part 118-1: synchrophasor for Power Systems - Measurements*, IEC/IEEE, Geneva, Switzerland, IEC/IEEE Standard 60255-118-1, Dec. 2018.

[34] *Instrument Transformers - Part 2: Additional Requirements for Current Transformers*, IEC, Geneva, Switzerland, IEC Standard 61869-2:2012, 2012.

[35] *Instrument Transformers - Part 3: Additional Requirements for Inductive Voltage Transformers*, IEC, Geneva, Switzerland, IEC Standard 61869-3:2011, 2011.

[36] A. Saber, A. Emam, and H. Elghazaly, “A backup protection technique for three-terminal multisection compound transmission lines,” *IEEE Trans. Smart Grid*, vol. 9, no. 6, pp. 5653–5663, Nov. 2018.

Ahmed Saber received the B.Sc., M.Sc., and Ph.D. degrees in electrical power engineering from Cairo University, Giza, Egypt, in 2008, 2013, and 2019, respectively. He was a Postdoctoral Fellow with Khalifa University, Abu Dhabi, UAE. He is currently an Associate Professor with Electrical Power Engineering Department, Faculty of Engineering, Cairo University. His research interests include HVAC and HVDC transmission system protection, AC microgrid protection, and hybrid AC/DC microgrid protection.

H. H. Zeineldin (Senior Member, IEEE) received the B.Sc. and M.Sc. degrees in electrical engineering from Cairo University, Giza, Egypt, in 1999 and 2002, respectively, and the Ph.D. degree in electrical and computer engineering from the University of Waterloo, Waterloo, ON, Canada, in 2006. He was with Smith and Andersen Electrical Engineering, Inc., North York, ON, where he was involved in projects involving distribution system designs, protection, and distributed generation. He was a Visiting Professor with the Massachusetts Institute of Technology, Cambridge, MA, USA. He is currently with the Khalifa University of Science and Technology, Abu Dhabi, UAE, and on leave from the Faculty of Engineering, Cairo University. His research interests include distribution system protection, distributed generation, and micro grids.

Ehab F. El-Saadany (Fellow, IEEE) was born in Cairo, Egypt, in 1964. He received the B.Sc. and M.Sc. degrees in electrical engineering from Ain Shams University, Cairo, Egypt, in 1986 and 1990, respectively, and the Ph.D. degree in electrical engineering from the University of Waterloo, Waterloo, ON, Canada, in 1998. He was a Professor with the ECE Department, University of Waterloo, till 2019. He was the Director of the Power MEng Program, University of Waterloo, during 2010–2015. He is currently a Professor with the Department of Electrical Engineering and Computer Science and the Director of the Advanced Power and Energy Research Center, Khalifa University, Abu Dhabi, UAE. He is a Registered Professional Engineer in the Province of Ontario. He is an internationally recognized expert in the area of sustainable energy integration and smart distribution systems. His research interests include smart grid operation and control, microgrids, transportation electrification, self-healing, cyber-physical security of smart grids, protection, power quality, and embedded generation. He is an IEEE Fellow for his contributions in distributed generation planning, operation and control.